



Research Paper / Makale

An Improved Design and Analysis of a Solar Receiver

Ömer Reşat ERSÖZ^a, Yunus ÇERÇİ^b, Orçun EKİN^{c*}

^{a,b,c}Mechanical Engineering Department, Adnan Menderes University, Aydın, Turkey
*orcun.ekin@adu.edu.tr

Received/Geliş: 16.04.2021

Accepted/Kabul: 27.07.2021

Abstract: In this study, a solar cavity heat receiver for a 36 m² two-axis parabolic dish collector has been designed, analyzed by employing computational fluid dynamics (CFD), manufactured in a local workshop and then tested experimentally on site. The receiver is an open type with a diameter of 624mm and a depth of 665mm and has a steel pipe spiral tubing with a helical tubing at the bottom. The diameter of the concentrated sunlight at the focal point was found to be 200 mm as a result of optical analysis with perfect mirror surface approach. The CFD model of the receiver, assuming the actual boundary conditions such as volumetric flow rate, input temperature of circulating water and line pressure showed that analyses approached the actual process, and also the process indicated that the analyses can be improved by taking into account the thermal radiation. Since for a period of approximately 30 minutes the system showed a steady-state characteristic during the daytime, a set of experimental measurements were carried out. It was found that the analytical outlet temperature was 1.07% higher than the experimentally measured outlet temperature and the numerical temperature was 0.15% higher than the experimental result.

Keywords: Computational fluid dynamics, Zenith and Azimuth Angles, Receiver, Concentrating Solar Power, Pipe Coiling

Gelişmiş Bir Güneş Kolektörünün Tasarımı ve Analizi

Öz: Bu çalışmada, 36 m² alana sahip iki eksenli bir parabolik çanak güneş kolektörü tasarlanmış, CFD yöntemleri ile analiz edilmiş, yerel bir atölyede üretilmiş ve sahada deneysel olarak test edilmiştir. Solar-kavite ısı alıcısı, bir tarafı açık silindirik bir kap olup, iç çapı 624mm ve derinliği 665 milimetredir. Silindirik yükseklik boyunca spiral bobinaj ve tabanında aynı borudan helisel bobinaj bulunur. Mükemmel ayna yüzey yaklaşımıyla yapılan optik analiz sonucunda yoğunlaştırılmış güneş ışığının odak noktasındaki çapının 200mm olduğu hesaplanmış, ancak bu çap değeri gerçek yüzeydeki kusurlar ve aynaların yönelimlerdeki küçük sapmalar sebebiyle spiral borunun dış çapına eşit alınmıştır. Sınır koşullarının hacimsel debi, suyun giriş sıcaklığı ve hat basıncına ait gerçek verilerle oluşturulduğu CFD modeli ile gerçekleştirilen analiz gerçek sistemin ölçüm verilerine yakınlık göstermiş olup, proses ısı ışınımının hesaplamalara dahil edilmesiyle analizlerin daha iyileştirilebileceğine işaret etmektedir. Sistemin yaklaşık 30 dakikalık bir süreçte gündüz saatlerinde kalıcı durum karakteristiği göstermesine dayanılarak, bir dizi ölçümler gerçekleştirilmiştir. Elde edilen analitik, nümerik ve deneysel veriler karşılaştırılmıştır. Analitik çıkış sıcaklığının deneysel sıcaklıktan 1.07% yüksek olduğu, hesaplamalı yöntem ile bulunan sıcaklığın deneysel sıcaklıktan 0.15% yüksek olduğu tespit edilmiştir.

Anahtar Kelimeler: Hesaplamalı Akışkanlar Dinamiği, Zenit ve Azimut Açılı, Kolektör, Güneş Enerjisi, Boru Bobinaj

1. Introduction

Public awareness on solar energy has been raised over the past years raised as a result of environmental catastrophes and imbalanced energy prices. Thermal energy production from concentrating sunlight offers a promising alternative to fossil energy and will lead to a significant

How to cite this article

Ersöz, Ö. R., Çerçi, Y., Ekin, O., "An Improved Design and Analysis of a Solar Receiver" El-Cezeri Journal of Science and Engineering, 2021, 8(3); 1272-1285.

Bu makaleye atıf yapmak için

Ersöz, Ö. R., Çerçi, Y., Ekin, O., "Gelişmiş Bir Güneş Kolektörünün Tasarımı ve Analizi" El-Cezeri Fen ve Mühendislik Dergisi 2021, 8(3); 1272-1285.
ORCID ID: *0000-0002-5751-8594; *0000-0002-4462-5366; *0000-0002-6779-885X

reduction off fossil fuel usage in global energy source preferences [1]. Being one of the most useful ways of energy production, gaining heat through concentrating sunlight to a point by a dish collector has been valued by the experts in the field [2]. The solar irradiation is converted by a solar dish to thermal energy on a regular base. This thermal energy is transferred in order to be used as circulation for heat transfer fluids. Three significant parts of a solar dish collector is listed as a receiver/absorber, tracking system and highly reflective mirrors with supporting body. The sunlight does not always enter the surface of mirrors parallel. Therefore, the experts design the reflected sunlight beams as a small image. Furthermore, it is still possible to occur unavoidable imperfections in the mirror positions as a result of heat expansion of the metal base, wind, etc. Therefore, it is created to be integrated for sunbeams as a small round shape instead of a perfectly focused point at the receiver of the system. The bigger the image is, the worse the concentration. [3]. Solar power plants might be considered as an alternative for world's fossil resources that are under the danger of extinction whereas they reduce the CO₂ emissions to the atmosphere in contrast to the fossil resources. [2]. Solar energy can be taken as the most efficient energy source because it is a clean renewable energy source and is possible to widely distributed [3]. There are many different ways of using solar radiation in the forms of power for heat engines, thermoelectric power generators (such as by Peltier elements or steam engines), photovoltaic cells for direct electricity production, crop drying, power for refrigerators and air conditioners, desalination of sea water and domestic hot water production [4-9]. Concentrating solar power (CSP) gets public attention in a wide extent and is thought as one of the most efficient alternatives [10]. In 2009 the world cumulative installed solar energy capacity was 22,928.9MW while there is a major change of 46.9% than the year of 2008 in accordance with the source of 2010 Statistical Energy Survey [11]. The CSP plants' overall operational capacity was published as about 4.7 GW by Desai and Bandyopadhyay [12].

One of the most significant features of CSP plants with line focus in concentrating solar collectors, similar to linear Fresnel collector and parabolic trough collector, are being simple in design and achieving temperature up to 400 °C. The CSP plants' total operational capacity is about 4.7GW. The most mature technology with about 87% of the worldwide operational CSP plants capacity is Parabolic trough collector (PTC) based CSP plant through using organic and synthetic oil for heat transfer fluid [13]. It is investigated by Pavlovic et al. (2017) a solar collector with a spiral absorber and dish reflector numerically and experimentally by a developed thermal model in the Engineering Equation Solver (EES). The investigation proved that the thermal performance was about 34%, because of the thermal losses' high ratio. They optically investigated an open receiver of a conical cavity in the shape of a helical tube in order to improve the receiver's optical performance. It is revealed that the helical conical shape with an aperture area of 0.01606 m² absorbed an average flux value of about 2.6 x 10⁵ W/ m² [8]. Another investigation has been run by Rafeu and Kadir (2012) used three experimental models with various geometrical sizes and solar dish concentrators with a diameter of about 0.5 m in order to search the geometry's effect on a solar temperature and irradiation by maximizing the solar fraction under the Malaysian environment. These models have been used to understand the performance of parabolic concentrating collector's parameters' performance such as aperture diameter, depth of concentrator, reflector materials, size of focal point and temperature at the focal point with various solar irradiations to enhance the thermal efficiency. It has been achieved that a major variation is possible in the concentrator's efficiency by using various reflective materials. It is proved that the efficiency of 3M Silver lux aluminum films is higher than the efficiency of stainless steel and it is possible to increase the results through enhancing the concentrator's area i.e., efficiency when comparing with the base [14].

Andrade et al. (2016) has conducted a research regarding the temporal temperature's behavior in a specimen located in a parabolic dish solar concentrator's focal point, and they proposed a dimension quantity (Ω). The diameter of the solar collector has been correlated with the solid mass to be heated and the rate of solar irradiance through their parameter, Ω . They investigated the

Equilibrium Temperature as a function of Ω . According to the results of their simulation, it is possible to achieve temperatures up to 1,600°C in relatively short periods of time, and it is proved that thermal energy for high temperature applications can be provided through the solar concentrator used in their study [15]. They assembled a solar cavity heat receiver at the parabolic reflector construction's focal point. There is a coiled tubing to convert the solar irradiation directly into thermal energy in the solar cavity heat receiver. Solar cavity heat receivers have been studied by various experts as shown in [16-15]. It is investigated by Azzouzi et al. (2017) the solar cylindrical cavity receiver's total heat loss and thermal efficiency for solar dish analytically and experimentally. Their downward facing receiver had a depth of 20 cm, inner diameter of 10 cm and 19 helically turns of copper tube. They based on an analytical model with its structure on the various Nusselt number correlations to analyze the radiative and convective heat losses by the cylindrical cavity. The total heat loss is possible to predict through their model in order to define the thermal efficiency of the receiver for a provided inclination angle [16].

It is developed by Kanatani et al. (2017) a solar cavity receiver model which uses helically coiled tubes as heat absorber. They calculated the coiled tube sand the heat transfer fluid's temperature distribution in the steady state. The maximum temperature of the coiled tubes, the pressure-drop, the receiver efficiency, the outlet temperature, the heat losses and the pumping power required for compressing the heat transfer fluid (air in this work) were approximately calculated. It is determined that if the receiver temperature is high or the total incident energy is small for the receiver temperature the efficiency decreases. Moreover, it is proved that the conductive heat loss through insulators around the coiled tubes is negligible among the total incident energy for that receiver configuration. The pumping power demand was small enough compared with the expected electric power output. It is concluded that the absorptivity of the receiver's ceiling could barely affect the outlet temperature as long as the absorptivity's difference between infrared and visible light of the coiled tubes and the conductive heat loss were not significant [17].

The effect of aspect ratio and head-on wind speed on the force and natural (combined) convective heat loss and area-averaged convective heat flux from a cylindrical solar cavity receiver are estimated through using three-dimensional computational fluid dynamics (CFD) simulations by Lee et al. (2017) They performed the cavity estimation while one end of the cavity is closed and the other end is open, assuming a uniform internal wall temperature. According to the numerical analysis, there were ranges of wind speeds for which the combined convective heat losses were lower than the natural convective heat loss from the cavity and this range is based on the cavity's aspect ratio. The wind speed's influence on the convective heat loss's area-averaged flux from a heated cavity was tinier for long aspect ratios than for short ones. This result showed the solar cavity receiver's overall efficiency raised with the aspect ratio for all conditions analyzed in that research [18]. It is stated by Reddy et al. [19] that the convective heat losses from the solar parabolic dish collector's modified cavity receiver numerically through focusing on the wind speed, wind direction, receiver orientation and receiver configuration. The inclinations of the receiver (0 to 90°), the wind's influence on the receiver in different directions (-90° to 90°), different surface temperatures on convective heat loss from the receiver and the operating wind speeds extending range (0–10 m/s) are investigated as a result of this study. They present temperature contours, velocity contours and vectors in order to prove the wind's influence on the heat loss from the modified cavity receiver. They observed that the forced convection had similar trend of free convection heat loss at lower wind speed while they have not experienced such a pattern at higher wind speed [19].

A survey, conducted by Samanes et al. [20] is based on the various natural convection correlations developed by different researchers to model the natural convective heat losses from the solar thermal power tower plants cavity receivers. A comparison has been made among the different

correlations investigated to model the convective heat losses through performing simulations on an implemented cavity receiver. It is proven that the four out of the five studied correlations' results complied with each other. However, one of the investigated correlations overestimated the convective heat losses for the simulations observed [20]. It is observed that data gathered through actual experimental measurements should provide realistic information as a time saving choice during the solar open cavity tubular heat receivers' performance analyses. In this paper it is suggested that comparison of the experimental measurements and numerical analysis's results together with the analytical calculation for the cavity receiver installed onto the manufactured and commissioned two-axis solar parabolic solar collector at the Central Campus, Adnan Menderes University. The numerical calculation in this study includes Fluent and analytic calculations involving heat flux applied on the pipe flow boundary surfaces and CFD analyses via ANSYS. Radiative and convectational energy transfer is ignored. Water is used as the circulating heating fluid in our study.

This study aims to build a correlation between a manufactured solar energy concentration system operating on the field and the relevant analytical approach in assessing the potential performance of such systems, by using CFD applications explicitly. Although similar studies where experimental-numerical comparison is adopted, the majority of those studies focus or heavily lean on the analytical methods in verifying theoretical heat transfer limits [21-24]. Bellos et al., discussed the heat transfer capabilities of cavity receivers, considering a variety of different coil geometries and using CFD [25]. Although a sweeping study, the most versatile scenario for a cavity receiver, which is the cylindrical configuration, has been overlooked in the said article, whereas the main focus of our study is the cylindrical configuration, with its process-dependent properties and detailed simulation.

2. Material and Method

Solar cavity heat receivers, which convert concentrated solar energy into heat, and transfer it to the operating fluid such as oil and water are an important component of solar dish collector applications. Although there are many different types of solar cavity heat receivers in the literature and practice, besides the designs that can minimize convection and radiation heat losses, and can take the entire amount of the concentrated solar energy into inside, the manufacturing limits and the diameter of the concentrated solar energy at the focal point have been among the significant parameters in the design progress.

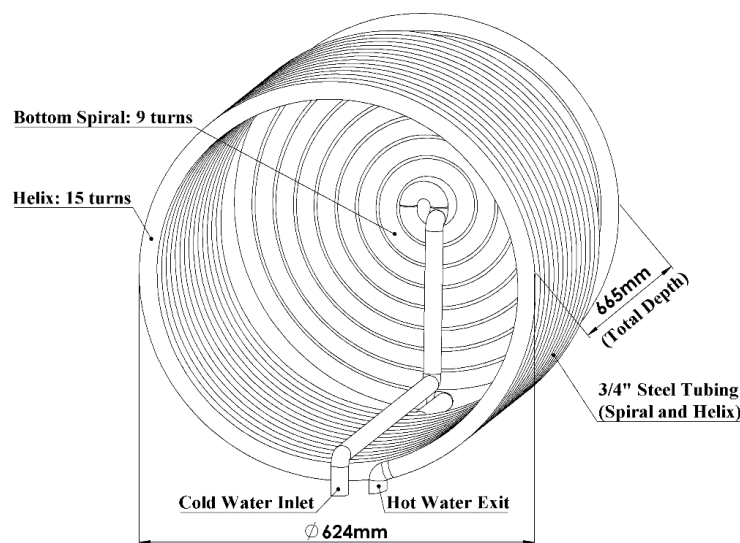


Figure 1. Solid modeling of cylindrical receiver with helical bottom.

The type of heat receiver chosen for this study is open cavity and it includes tubing in the cylindrical helical shape with flat helical on the base. Two important parameters were considered in the sizing of the heat receiver, which were the minimum bending diameter of the three-point bending machine and the diameter of the concentrated solar energy at the focal point of the tracking system. The minimum bending diameter of the three-point bending machine was found to be 624 mm, and thus this diameter was determined as the inner diameter of the heat receiver. Although the diameter of the concentrated solar energy, on the other hand, was figured out from optical analysis to be 200 mm, it was increased to the inner diameter of the cavity due to the defects on mirror reflector and orientation errors of the mirror facets. The size of the 3/4-inch steel and cylindrical helical tubing is 570 mm in height and 624 mm in diameter. The height of the receiver consists of 15 revolutions while the back wall of the receiver consists of 9 revolutions. The tube made of steel is a usual 3/4-inch tube mostly run for plumbing purposes consists of another diameter of 26.9 mm and an inner diameter of 21.1 mm. The spacing between coil turns is small and therefore the pitch is the same size with the tube’s outer diameter. With these dimensions, the receiver’s 3D solid modeling was created through using SolidWorks and shown in Figure 1. Also, Table 1 provides the receiver parameters.

Table 1. Specifications of cylindrical shaped with helical bottom receiver.

Coil Parameters	Values
Outer diameter of coil	624 mm
Inner tube diameter	21.1 mm
Outer tube diameter	26.9 mm
Length	27.78m (helix coil) 9.76m (bottom spiral)
The number of turns for the helix coil	15
The number of turns for the bottom spiral	9

The theoretical evaluation’s main goal is estimating the suitable solar energy obtained from the heat receiver through applying the principle of the conservation of energy to the receiver. Figuring out the beam radiation for the measurement time is the first step during the calculation. First, the heat receiver’s theoretical evaluation begins with the direct normal beam radiation’s calculation on August 15th that was the measurement day. The observation was made at 15:45 local time. The time and beam radiation were calculated as 288 W/m² on that day by solar energy equations’ series. All other values are shown in Table 2. All values excluding the beam radiation were measured experimentally.

Table 2. Solar radiation and system related values for the day of measurement.

Location	Aydın (37.85°, 27.85°)
Date	August 15
Time	15:45 (Local Time)
Beam radiation	288 W/m ²
Mass flow rate of water	0.392 kg/s
Inlet velocity of water	1.12 m/s
Inlet temperature of water	42.9 °C
Outlet Pressure of water	5 Atm

Although the mirrors total surface area is 36 m² but there are 4 cm space between the mirrors to implement the wind flow in order to extend the platform’s endurance under extraordinary climate conditions. If the spaces between the mirrors are eliminated, there is a net 28 m² mirror area. The

beam radiation strikes at the 28 m² parabolic reflective mirror and fixated normal to the heat receiver’s cross-sectional area, that is named as receiver aperture area, represented in Equation 1:

$$C_a = A_{conc}/A_{rec} \tag{1}$$

where the concentration ratio (C_a) must be figured out first in order to calculate the heat flux coming on to the receiver. Also, the geometric concentration ratio is generally defined as the concentrator aperture area (A_{conc}) to the receiver aperture area (A_{rec}) [3]. In this study, the equation mentioned above provides the concentration ratio as 93.3; taking the receiver aperture area of 0.3 m². Assuming the reflectivity of aluminum coated plastic mirrors as 0.9, it reveals that the total heat flux coming to the receiver is calculated as 24,183 W/m². Both the numerical and analytical analysis can be based on this value.

The useful solar energy provided through the heat receiver can be defined by employing the following simple energy equation below:

$$\dot{Q}_u = \dot{m}c_p(T_o - T_{in}) \tag{2}$$

where \dot{Q}_u is the useful energy per second (power) delivered from the heat receiver (W), \dot{m} is the mass flow rate of water (kg/s), c_p is the specific heat of water (kJ/kg °C), T_{out} is the outlet water temperature, and T_{in} is the inlet water temperature. According to the direct normal beam and the concentration ratio, also when the receiver absorbs all the concentrated energy, with an effective absorptivity of 0.7, the water’s outlet temperature can be calculated from Equation 2 analytically. Our analytical results obtained from Equation 2 is shown in Table 3.

Table 3. Analytical results.

Parameters	Values
Solar flux	24,183 W/m ²
Useful heat gain	4340 W
Inlet temperature of water	42.9 °C
Outlet temperature of water	45.99 °C

The model’s CFD analysis is performed through using ANSYS Fluent. Both the cavity receiver’s 3D tubing modeling and the only water volume in tubing is examined in our numerical modeling. The model created in SolidWorks CAD environment is transferred to ANSYS meshing.

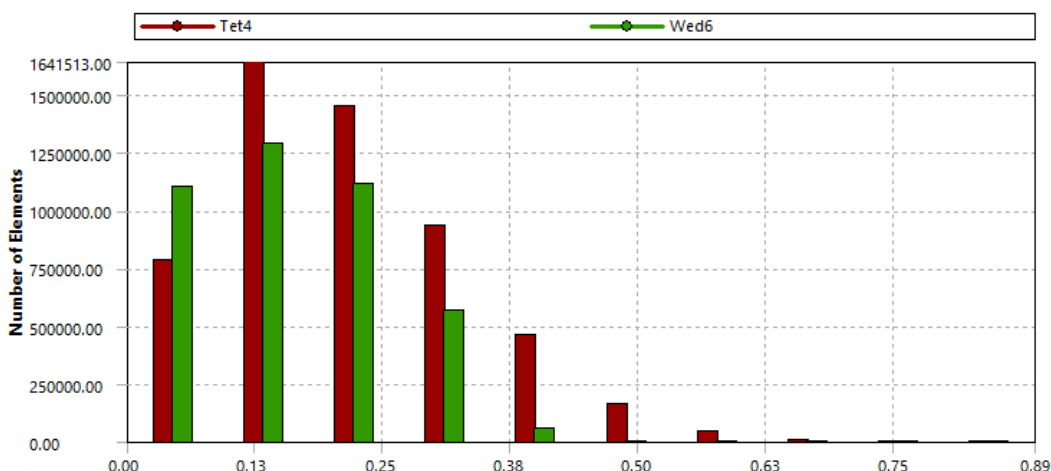


Figure 2. Mesh skewness with the average value is 0.1922, approximately.

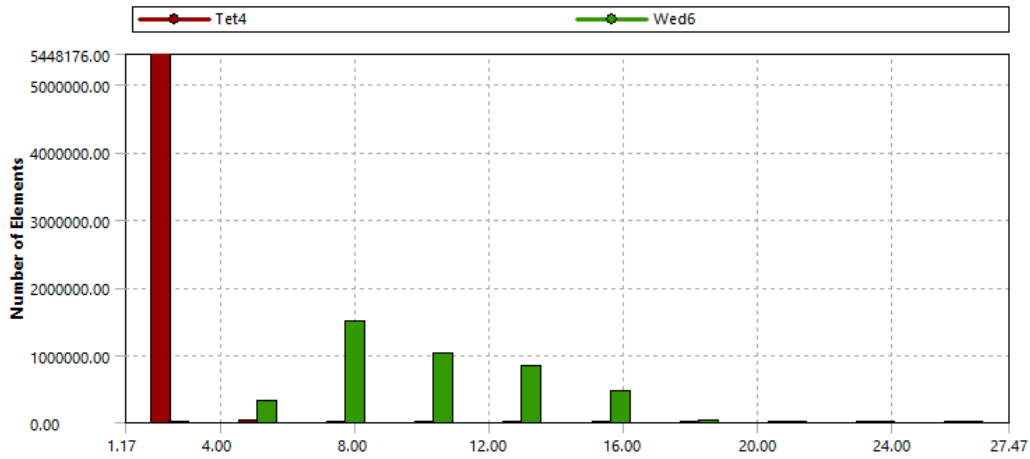


Figure 3. Mesh aspect ratio, with a 5.364 average (due to the contribution of wedge elements).

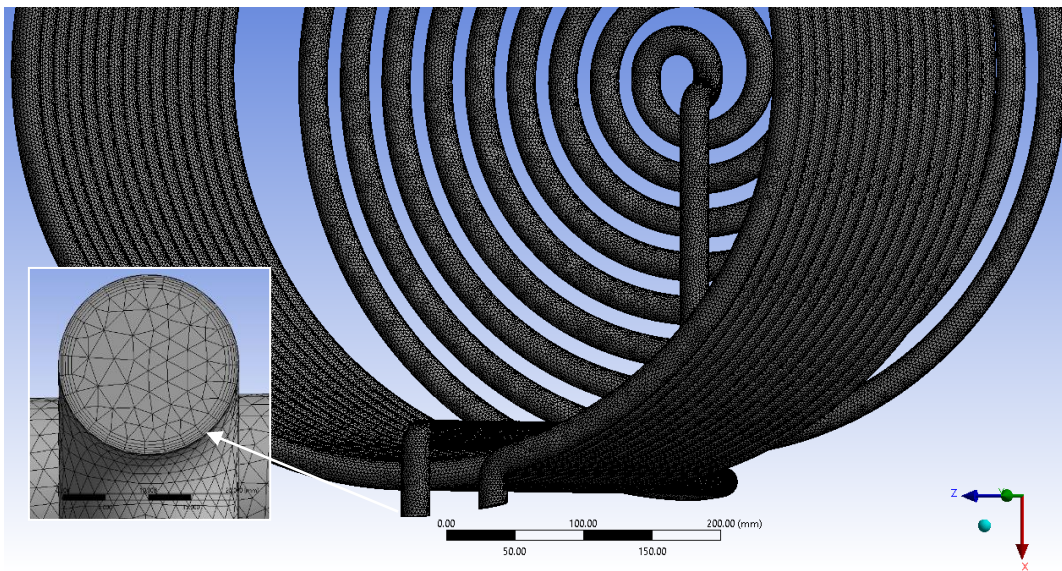


Figure 4. Mesh overview with the application of inflation layers.

The meshed model geometry mostly consists of tetrahedrons in that there are 3,192,591 nodes and 9,588,068 elements with a minimum edge length of 66.3 mm. The solution’s convergence and certainty for the model is examined for orthogonal quality and skewness, which should not outpace certain amounts. Mesh skewness, as a rule of thumb is best limited to 0.95 with an average of below 0.33. Aspect ratio, on the other hand, should be close to an average value of 1, in order to provide a good proportion of long dimension to short dimension of an element. In our mesh structure, skewness (Figure 2) and aspect ratio (Figure 3) statistics are well within those definitions, promising a successful validation against the experimental values.

The fluid dynamics analysis and computational heat transfer begin with the boundary conditions definition for the helical tube. It is better to examine only the flowing water domain excluding the steel tube itself for simplicity and by the benefit of hindsight. The beam radiation striking on to receiver tube is considered as the heat flux applied on to the water domain wall and normalized along the helical tube’s length. The outlet and the inlet for the domain are defined as pressure outlet and velocity inlet. The numerical values for the input parameters are provided in Table 2. The general settings of the CFD analysis were steady and pressure-based. Gravity, turbulence model, and wall treatment were chosen to be 9.82 m/s², standard k-epsilon, and standard wall function, respectively.

Density, specific heat, and thermal conductivity of water were 998.2 kg/m^3 , 4.182 kJ/kg K , and 0.6 W/m K , respectively. The value entered for the scaled residuals were 1×10^{-5} . As a result of numerical analysis under these conditions, the water outlet temperature was determined to be $45.57 \text{ }^\circ\text{C}$. The cylindrical helical tube designed together with flat spiral tube was produced in accordance with the model explained previously and installed an insulated cylindrical container. Figure 5 is the cavity receiver's photo in this study.



Figure 5. A photo of the solar cavity receiver.

3. Results

Figure 6 shows a receiver's typical thermal camera image. It is clearly seen from the figure that the helical coils inside the receiver have the maximum surface temperatures from $45.99 \text{ }^\circ\text{C}$ to $79.5 \text{ }^\circ\text{C}$. The measured outlet water temperature was $45.5 \text{ }^\circ\text{C}$ which is very close to the theoretically calculated results obtained by analytic and numerical calculations (Figure 6).

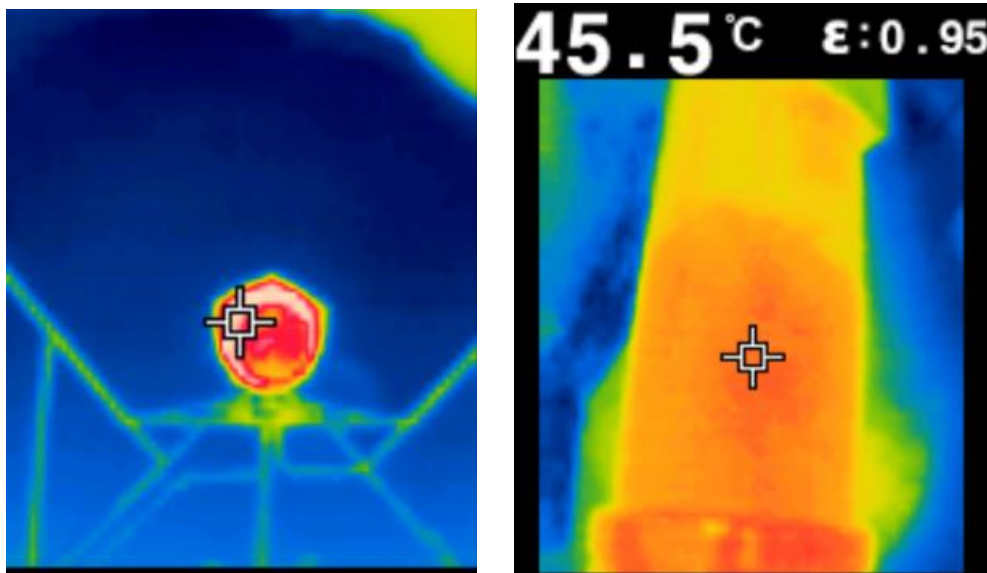


Figure 6. Thermal camera image of the receiver, (left) brighter colors indicating higher temperatures, (right) the water outlet temperature

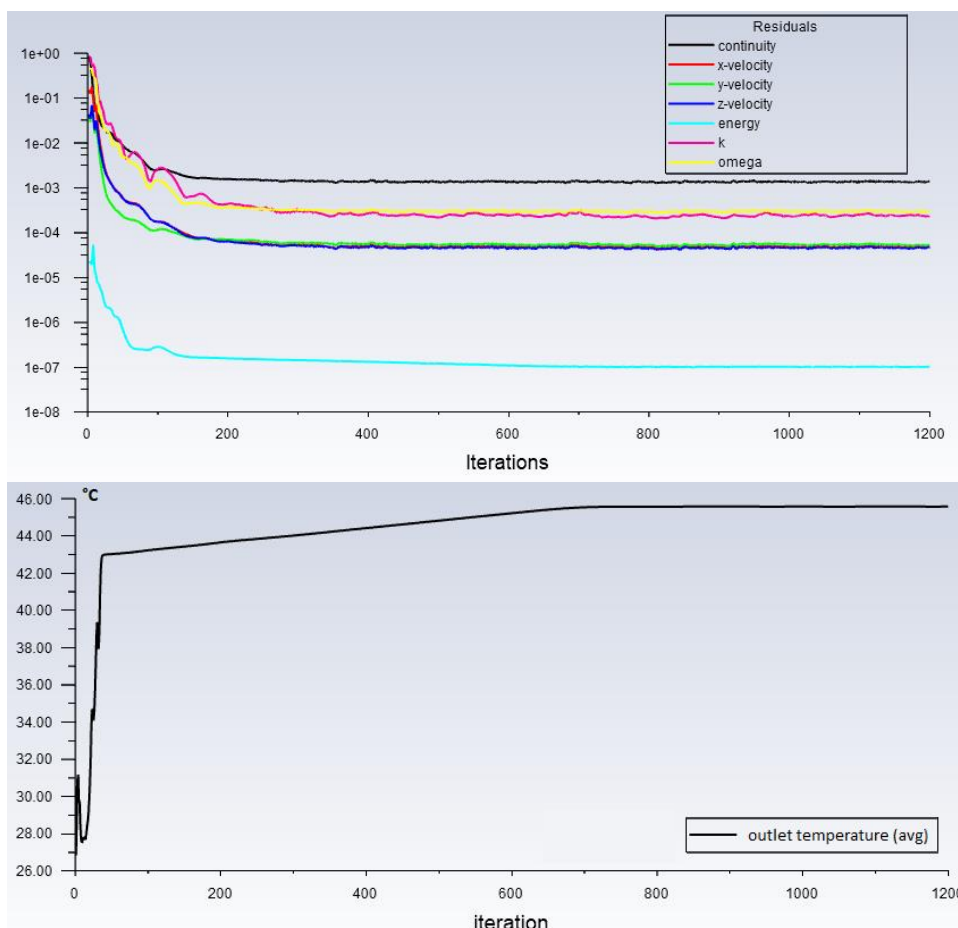


Figure 7. Scaled residuals (above) and mass flow stabilization (below) in ANSYS Fluent Solver.

Analytical, numerical, and experimental results are tabulated in Table 4. The analytical, numerical, experimental water outlet temperatures are 45.99°C, 45.57°C, and 45.5°C, respectively. The analytical temperature is 1.07% higher than the experimental temperature, whereas the CFD results suggest a 0.15% relative error when compared to the experimental value, which indicates a reliable validation point. These results clearly direct us to confirm that the analytical model is reliable, but the numerical model needs to be improved by performing further modifications.

The results of the scaled residuals and the stability of the outlet temperature are shown in Fig 7. Due to the total number of elements (tetragonal and wedge) the analysis consumes up to 8 hours. When the k-omega turbulence model parameters are considered, Continuity displays a poor convergence, at 1e-03 relative error, whereas the other parameters all drop below 5e-05. Although the time consumption of the current model cannot be easily neglected, the convergence characteristics are adequate for the average outlet temperature to stabilize at a relatively small number of 700 iterations.

In any practical heat transfer analysis, three types of heat transfer mode can be considered; conduction, convection and radiation [26, 27]. These three modes of heat transfer sum up to total heat transfer rate coinciding a surface as in Equation 3:

$$\dot{Q} = \dot{Q}_{cond} + \dot{Q}_{conv} + \dot{Q}_{rad} \tag{3}$$

Where \dot{Q}_{cond} , \dot{Q}_{conv} and \dot{Q}_{rad} are the rate of conduction, convection and radiation heat transfer, respectively with \dot{Q} representing the overall rate of heat transfer. Regarded result of being the most

general solution of any heat transfer phenomenon, effects of these modes' influences can be ignored, or multiple modes can be neglected, in accordance with the application being taken. In our analytical calculations, only a constant heat flux acting on the entire coil (spiral and helix parts) surface, as convective heat transfer and a radiative modes' lumped parameter, is considered. The heat flux's magnitude is described through the procedure mentioned in the previous sections beam radiation, corresponding the cavity receiver's inlet opening, as defined above. In the actual process, examined as a closed-loop cycle, rock wool insulator is utilized to wrap piping by the installation, the thickness of that is measured through taken critical insulation radius. Therefore, it is assumed that there is not any heat lost from water flowing inside the pipe to the environment. Radiation heat transfer coming from a distant source is interpreted very similarly to analytical approach into a simpler approach and constant heat flux is covered to the coil surface (bottom spiral and cylindrical helix components).

The results of distribution and gradual increase of temperature at the coiling's spiral component is provided in Figure 8. As expected, the temperature at the inlet surface, which was measured on the day of field experiments to be 42.9°C gradually increases through the distance of coiling. However, faint on the volume rendering option (left), the slight temperature drop at the vicinity of the outlet surface can be observed on the temperature contour graph of the coiling wall.

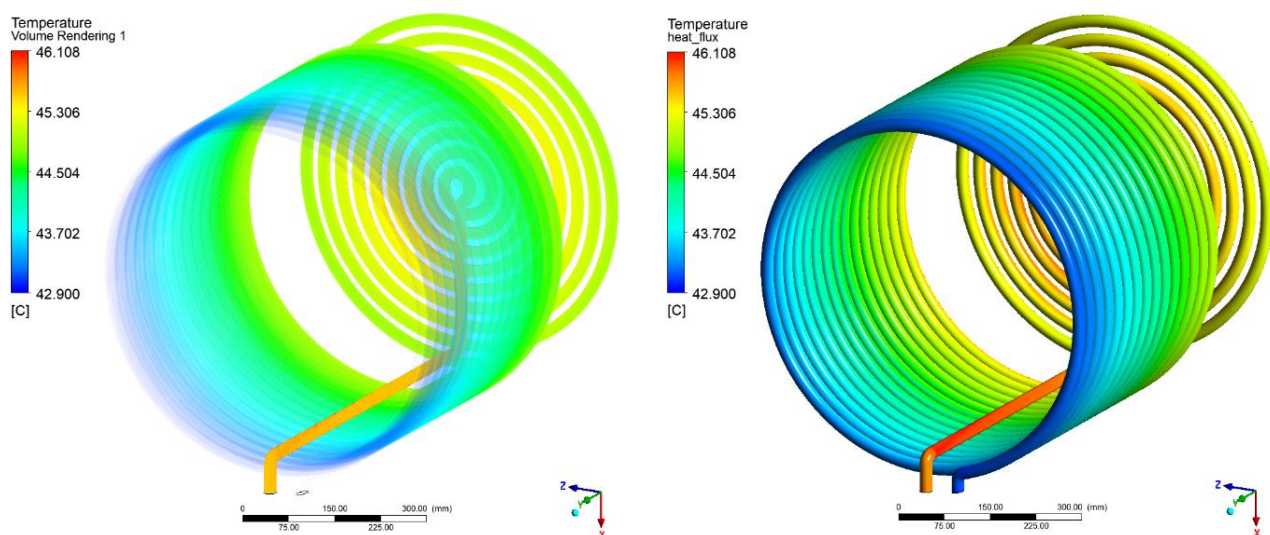


Figure 8. Heat admission and temperature rise in piping (left), inner wall temperature (right).

A streamline graph was utilized for the velocity visualization through the coiling. A volume average 1.136 m/s can be calculated, with peak values reach 2.2 m/s . One of those parts where the velocities exceeding the average are observed at the 90° elbow couplings at spiral-outlet tube connection zone of the coiling. A detailed streamline graph can be seen on the bottom of Figure 9 where small eddies are present near the both connection areas of the elbows. Similar irregularities in fluid flow were observed at locations where the monotonous geometry (i.e., the curvature) is changed.

The inlet mass flow rate boundary condition measured on the day of field testing suggests a fully developed flow velocity of 1.12 m/s which results in a Reynolds number of 2.37×10^4 through $3/4''$ steel pipe, indicating transition flow. The Standard k-omega turbulence model was selected based on this initial calculation, after which an inflation is applied to the existing geometry. On Figure 10, the mesh structure with the addition of inflation layers (total thickness, first layer thickness) can be

seen. It can be suggested that the asymmetric temperature map on Figure 10 is a probable cause of the effect of gravity.

Finally, the CFD results offer a valid basis for heat transfer assessment through the coiling model, specifically for the current application, when compared to the experimental data. The significant difference between the analytical and experimental data on the other hand, could be the effect of the ideal conditions adopted when calculating the output temperature i.e., no heat lost from the cavity receiver due to convection or shell conduction through the wall of coiling tube. The results comparison of the three methods of measurement are briefly summarized on Table 4.

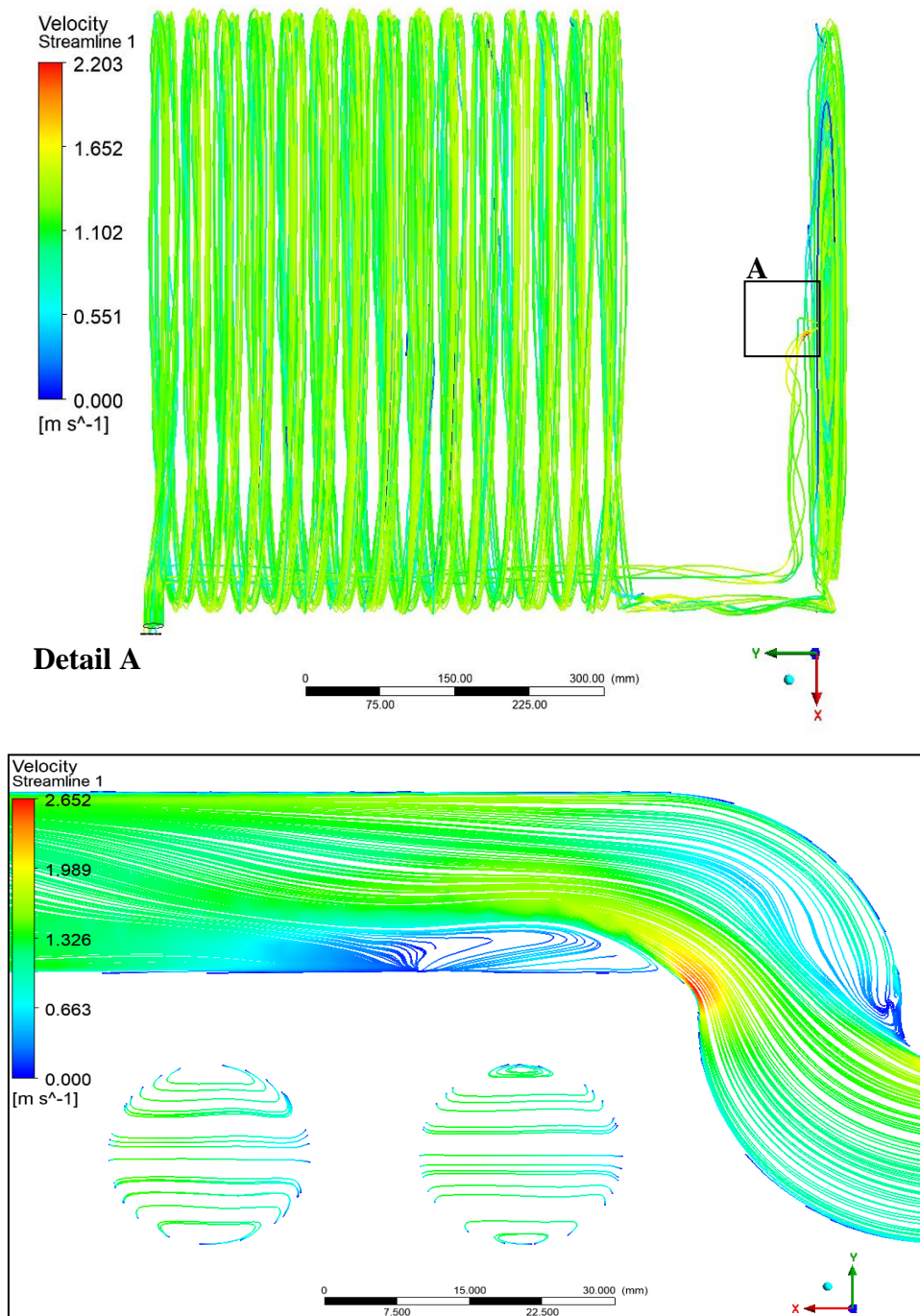
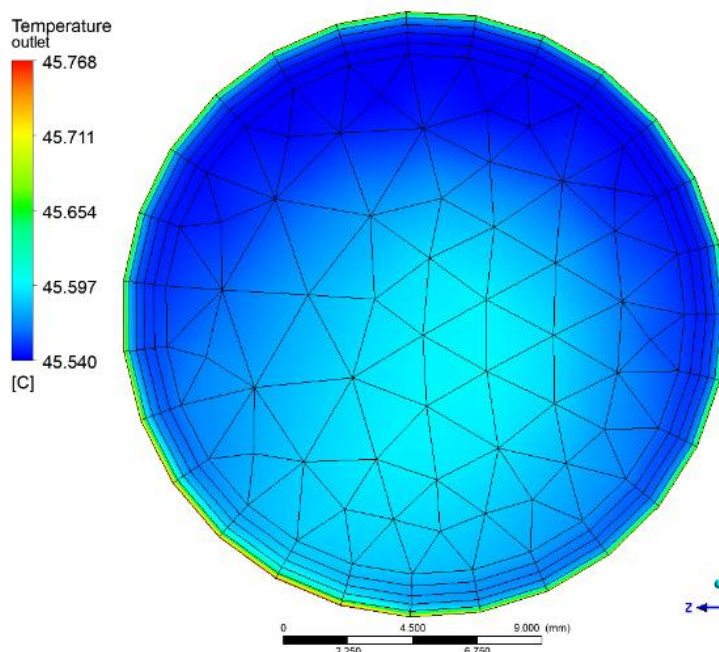


Figure 9: (Top) The overall streamline graph of flow through coiling. (Bottom) Detail “A” of streamline and eddy occurrences at the outlet of the bottom spiral (color chart indicates the local velocities on the cross-sectional plane).

Table 4. Outlet temperature of water

Parameter	Analytical	CFD	Experimental
Water Temperature (on the Outlet)	45.99 °C	45.57 °C (Area Averaged)	45.5°C

**Figure 10.** CFD-post outlet velocity distribution cross section.

4. Conclusion

A solar cavity heat receiver's inner tubing that is mostly used in concentrated solar energy collectors is created, produced, and examined experimentally in this study. We model the inner tubing as flat helical on the base and cylindrical helical on the lateral surfaces and manufacture accordingly. Theoretically calculated solar beam radiation value on August 15th at 15:45 (Local Time) of the experimental measurement was used in the analytical calculations and numerical analysis. Experimental, analytical and numerical studies have proven that the water outlet temperature is 45.5°C, 45.99°C and 45.57°C respectively. The fact that the water outlet temperatures are relatively close within a percentage ranging from 0.15 % to 1.07% to the experimentally measured temperature where the cumulated effect of all modes of heat transfer naturally adopted as a result of infrared measurement, reveals that the numerical and analytical models are similar to reality. It proves that the receiver is protected well. Specified analysis research including the thermal energy transfer's other forms on the numerical and analytical modeling of this work is improving and is expected to be completed in the following term of the study.

Acknowledgments

The authors would like to thank BAP Department of Aydın Adnan Menderes University for the resources provided. This study was funded under the Project No 18015.

Authors' Contributions

All authors contributed to the article evenly. Also, the authors read and approved the final manuscript.

Competing Interests

The authors declare that they have no competing interests.

References

- [1]. Kumar, A., Prakash, O., Kaviti, A., K., A Comprehensive Review of Scheffler Solar Collector, *Renewable and Sustainable Energy Reviews*, 2017 (77), 890-898.
- [2]. Tan, Y., Zhao, L., Bao, J., Liu, Q., Experimental Investigation on Heat Loss of Semi-spherical Cavity Receiver, *Energy Conversion and Management*, 2014, (87), 576-583.
- [3]. Li, H., Huang, W., Huang, F., Hu, P., Chen, Z., Optical Analysis and Optimization of Parabolic Dish Solar Concentrator with a Cavity Receiver, *Solar Energy*, 2013 (92), 288-297.
- [4]. Kurup, P., Turchi, C., Initial Investigation into the Potential of CSP Industrial Process Heat for the South West United States, National Renewable Energy Laboratory, USA.
- [5]. Bahçeci, S., Daldaban, F., Dağıtım Şebekelerinde Güneş Panelleri ve Enerji Depolama Uygulaması, *El-Cezerî Journal of Science and Engineering*, 2017 (4), 308-313.
- [6]. Alcan, Y., Demir, M., Duman, S., Sinop İlinin Güneş Enerjisinden Elektrik Üretim Potansiyelinin Ülkemiz ve Almanya ile Karşılaştırılarak İncelenmesi, *El-Cezerî Journal of Science and Engineering*, 2018 (5), 35-44.
- [7]. Çelen, S., Arda, S. O., Karataşer, M. A., Güneş Enerji Destekli Mikrodalga Konveyör Kurutucu Kullanılarak Kuruma Davranışının Modellenmesi, *El-Cezerî Journal of Science and Engineering*, 2018 (5), 267-271.
- [8]. Tan, F., Shojaei, S., Past to Present: Solar Chimney Power Technologies, *El-Cezerî Journal of Science and Engineering*, 2019 (6), 220-235.
- [9]. Kırbas, İ., Çifci, A., Feasibility Study of a Solar Power Plant Installation: A Case Study of Lake Burdur, Turkey, *El-Cezerî Journal of Science and Engineering*, 2017 (6), 830-835.
- [10]. Desai, N. B., Bandyopadhyay, S., Nayak, J.K., Banerjee, R., Kedare, S. B., Simulation of a 1MWe Solar Thermal Power Plant, *Energy Procedia*, 2014 (57), 507-516.
- [11]. Solangi, K.H, Islam, M. R., Saidur, R., Rahim, N. A., Fayaz, H., A Review on Global Solar Energy Policy, *Renewable and Sustainable Energy Reviews*, 2011 (15), 2149-2163.
- [12]. Desai, N. B., Bandyopadhyay, S., Thermo-economic Comparisons Between Solar Steam Rankine and Organic Rankine Cycles, *Applied Thermal Engineering*, 2016 (105), 862-875.
- [13]. Pavlovic, S., Daabo, A. M., Bellos, E., Stefanovic, V., Mahmoud, S., Al-Dabah, R. K., Experimental and Numerical Investigation on the Optical and Thermal Performance of Solar Parabolic Dish and Corrugated Spiral Cavity Receiver, *Journal of Cleaner Production*, 2017 (150), 75-92.
- [14]. Rafeeu, Y., Kadir, M. Z. A., Thermal Performance of Parabolic Concentrators Under Malaysian Environment: A Case Study, *Renewable and Sustainable Energy Reviews*, 2012 (16), 3826-3835.
- [15]. Andrade, L.A., Barrozo, M.A.S., Vieira, L.G.M., A Study on Dynamic Heating in Solar Dish Concentrators, *Renewable Energy*, 2016 (87), 501-508.
- [16]. Azzouzi, D., Boumeddane, B., Abene, A., Experimental and Analytical Thermal Analysis of Cylindrical Cavity Receiver for Solar Dish, *Renewable Energy*, 2017 (106), 111-121.
- [17]. Kanatani, A., Yamamoto, T., Tamaura, Y., Kikura, H., A Model of a Solar Cavity Receiver with Coiled Tubes, *Solar Energy* 2017 (153), 249–261.
- [18]. Lee, K. L., Jafarian, M., Ghanadi, F., Arjomandi, M., Nathan, G., An Investigation into the Effect of Aspect Ratio on the Heat Loss from a Solar Cavity Receiver, *Solar Energy*, 2017 (149), 20-31.
- [19]. Reddy, K. S., Veershetty, G., Vikram, T. S., Effect of Wind Speed and Direction on Convective Heat Losses from Solar Parabolic Dish Modified Cavity Receiver, *Solar Energy*, 2016 (131), 183-198.

- [20]. Samanes, J., Garcia-Baberena, J., Zaversky, F., Modeling Solar Cavity Receivers: A Review and Comparison of Natural Convection Heat Loss Correlations, *Energy Procedia*, 2015 (69), 543-552.
- [21]. Zou, C., Zhang, Y., Falcoz, Q., Neveu, P., Li, J., Zhang, C., Thermal Modeling of a Pressurized Air Cavity Receiver for Solar Dish Stirling System, *AIP Conference Proceedings*, 2017, 18-50.
- [22]. Loni, R., Ardeh, E. A. A., Ghobadian, B., Bellos, E., Numerical investigation of a solar dish concentrator with different cavity receivers and working fluids, *Journal of Cleaner Production*, 2018 (198).
- [23]. Yang, S., Wang, J., Lund, P., Wang, S., Jiang, C., Reducing convective heat losses in solar dish cavity receivers through a modified air-curtain system, *Solar Energy*, 2018 (166), 50-58.
- [24]. Bopche, S.B., Kumar, S., Experimental Investigations on thermal performance characteristics of a Solar Cavity Receiver, *International Journal of Energy and Environmental Engineering*, 2016 (10), 463-481.
- [25]. Bellos, E., Bousi, E., Tzivanidis, C., Pavlovic, S., Optical and thermal analysis of different cavity receiver designs for solar dish concentrators, *Energy Conversion and Management*, 2019 (10-2).
- [26]. Barbosa, F., Afonso, J. L., Rodrigues, F. B., Teixeira, J., Development of a Solar Concentrator with Tracking System, *Mechanical Science*, 2016 (7), 233–245.
- [27]. Gorjan, S., Hashjin, T. T., Ghobadian, B., Thermal Performance of a Point-focus Solar Steam Generating System, *Proceedings*, 21st Annual International Conference on Mechanical Engineering, ISME, 2013.